Check for updates

View Article Online
View Journal

Dalton Transactions

Accepted Manuscript

This article can be cited before page numbers have been issued, to do this please use: C. Zhang, K. Qiu, C. Liu, H. Huang, T. W. Rees, L. Ji, Q. Zhang and H. Chao, *Dalton Trans.*, 2018, DOI: 10.1039/C8DT02918K.

This is an Accepted Manuscript, which has been through the Royal Society of Chemistry peer review process and has been accepted for publication.

Accepted Manuscripts are published online shortly after acceptance, before technical editing, formatting and proof reading. Using this free service, authors can make their results available to the community, in citable form, before we publish the edited article. We will replace this Accepted Manuscript with the edited and formatted Advance Article as soon as it is available.

You can find more information about Accepted Manuscripts in the author guidelines.

Please note that technical editing may introduce minor changes to the text and/or graphics, which may alter content. The journal's standard Terms & Conditions and the ethical guidelines, outlined in our author and reviewer resource centre, still apply. In no event shall the Royal Society of Chemistry be held responsible for any errors or omissions in this Accepted Manuscript or any consequences arising from the use of any information it contains.

ROYAL SOCIETY OF CHEMISTRY

rsc.li/dalton

Please do not adjust margins
View Article Online
DOI: 10.1039/C8DT02918K

Journal Name

ARTICLE

Tracking mitochondrial dynamics during apoptosis with phosphorescent fluorinated iridium(III) complexes†

Received 00th January 20xx,
Accepted 00th January 20xx

DOI: 10.1039/x0xx00000x

www.rsc.org/

Chen Zhang,‡[a] Kangqiang Qiu,‡[ab] Chaofeng Liu,[a] Huaiyi Huang,[a] Thomas W. Rees,[a] Liangnian Ji,[a] Qianling Zhang,*[b] and Hui Chao*[ab]

Mitochondria are the control centers of apoptosis. To study mitochondrial dynamics during apoptosis, four phosphorescent fluorinated iridium(III) complexes (**Ir1-Ir4**) were designed and synthesized. The complexes emission maxima phosphorescent quantum yields, and phosphorescent lifetimes are tuned by the degree of fluorination of the ligand. The complexes exhibit excellent photostability and low (photo)cytotoxicity in HeLa cells. As the complexes are cationic and lipophilic, they localize in mitochondria and enter cells through an energy-independent pathway. In comparison with commercially available mitochondrial trackers MTR, Ir1-Ir4 exhibit high specificity to mitochondria even in fixed cells. Due to these outstanding properties, the complexes were successfully used to track mitochondrial dynamics during apoptosis.

Introduction

Apoptosis (from the Greek word for leaves falling off trees), was first used to describe natural cell death in the 19th century by embryologists and anatomists.[1-3] It is prevalent in eukaryotes,[4,5] which could keep the balance between new-generating cells from mitosis and cell death.[6] Apoptosis defects can cause a variety of malignant diseases, even cancer.[7] The key to triggering or inhibiting apoptosis lies in the mitochondria.[9,10] Mitochondria are the powerhouse of cells[11-13] and their protein-related modulation of apoptosis has two modes, the release or activation of caspase[14,15] and the signal transmission of Bcl-2 family stimuli.[16,17] The morphologies of mitochondria can change during apoptosis and differ from normal states.[18-20] Moreover, the mitochondrial morphologies are also different in different stages of apoptosis.[21-23] To study the relationship between mitochondrial morphologies and apoptosis, it is of great importance to track mitochondrial dynamics during apoptosis.

For biological dynamics tracking, the probes must exhibit low cytotoxicity and superior photostability.[24-26] Organic dyes have been used as mitochondria imaging agents, even commercially. But most of them are limited in tracking because of poor photostability.[27,28] Metal-based complexes could largely overcome photobleaching because of their structural properties.[29-31] Among them, phosphorescent Ir(III) complexes have been shown as promising candidates for bio-imaging.[32-35] Compared to commercial dyes, Ir(III) probes possess the advantages of lower cytotoxicities, stronger phosphorescence intensities, longer phosphorescent lifetimes and good photostabilities.[29-39] Cationic Ir(III) complexes are particularly of interest as they can specifically target mitochondria due to the mitochondrial membrane potential of -180 mV.[25,26,31,40] However, most reported mitochondria-targeting Ir(III) cations have a $[Ir(C^N)_2(N^N)]^+$ architecture, mitochondria-targeting terpyridyl Ir(III) complexes with a $[Ir(N^N^N)(C^N)Cl]^+$ structure are rare (Fig. 1).[41,42]

Fluorocarbons have attracted tremendous attention in biological applications due to their properties such as lipophobicity, hydrophobicity and bioinertness.[43-45] Interestingly, the good biocompatibility and low toxicity of fluorinated compounds has been reported in biological systems.[46-48] Herein, a series of terpyridyl Ir(III) complexes (**Ir1-Ir4**) with different fluorine atoms were designed and synthesized (Fig. 2) for tracking mitochondrial dynamics during apoptosis. The photophysical properties of the fluorinated complexes were studied in solution and in cells. With low cytotoxicities, excellent photostability and the ability to

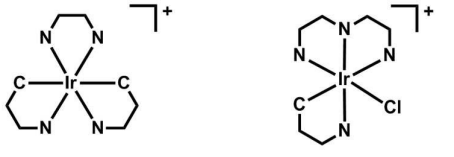

Fig. 1 Two types of Ir(III) architectures.

[a] MOE Key Laboratory of Bioinorganic and Synthetic Chemistry, School of Chemistry, Sun Yat-Sen University, Guangzhou, 510275, P. R. China.
[b] College of Chemistry and Environmental Engineering, Shenzhen University, Shenzhen, 518055, P. R. China.
Email: ceschh@mail.sysu.edu.cn (H. Chao); zhql@szu.edu.cn (Q. Zhang).
‡ These authors contributed equally to this work.
† Electronic supplementary information (ESI) available: additional data. See DOI: 10.1039/x0xx00000x

Published on 07 August 2018. Downloaded by University of Sussex on 8/9/2018 9:27:02 AM.

Dalton Transactions Accepted Manuscript

View Article Online
DOI: 10.1039/C8DT02918K

Published on 07 August 2018. Downloaded by University of Sussex on 8/9/2018 9:27:02 AM.

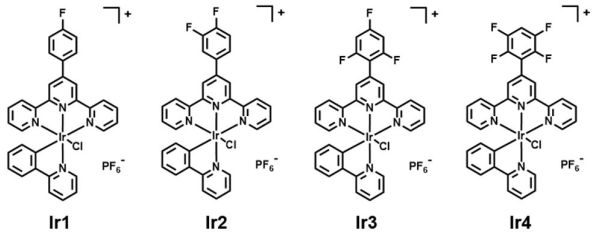

Fig. 2 The chemical structures of the iridium complexes **Ir1-Ir4**.

specificity target mitochondria, the complexes were developed as mitochondrial probes for real-time tracking of mitochondrial dynamics during the early stages of apoptosis. The uptake mechanisms of the complexes were also investigated in detail.

Results and discussion

Design and synthesis

The complexes were synthesized through the synthetic route (Scheme S1). The fluorinated terpyridyl ligands were obtained firstly. Then **Ir1-Ir4** were synthesized by reacting $IrCl_3 \bullet 3H_2O$ and the corresponding ligands in ethylene glycol *via* a two-step reaction. The Ir(III) complexes were purified by alumina column chromatography with eluents of acetonitrile and toluene, and characterized with elemental analysis, ES-MS (Fig. S1-S4), ^{1}H NMR (Fig. S5-S8) and ^{19}F NMR (Fig. S9-S12).

Photophysical properties

The photophysical properties of **Ir1-Ir4** at 298 K in phosphate buffer saline (PBS) were performed (Fig. 3) and the data were presented in Table S1. A weak absorption was found around 470 nm in the UV-Vis spectra and an intense absorption was observed at 300-400 nm.[49] When excited at 405 nm, **Ir1-Ir4** exhibit yellow to orange phosphorescent emissions from 549 to 569 nm. The wavelengths of emission peaks showed a red shift when the number of F atoms increased. The phosphorescent lifetimes of the complexes are 731 ns (**Ir1**), 655 ns (**Ir2**), 511 ns (**Ir3**) and 400 ns (**Ir4**). Using $[Ru(bpy)_3]^{2+}$ as a standard, the quantum yields of **Ir1-Ir4** in PBS buffer were measured as 14.3 %, 12.7 %, 9.23 % and 5.56 %, respectively.[50] The change in phosphorescent lifetime and quantum yields could be attributed to variations of dipole moment and electron distribution within the complexes, which due to the electron withdrawing influence of F.[51] Furthermore, **Ir1-Ir4** displayed superior photostablity in buffer solution (Fig. S13) during continuous irradiation for 40 minutes, which is a desirable property for practical applications.

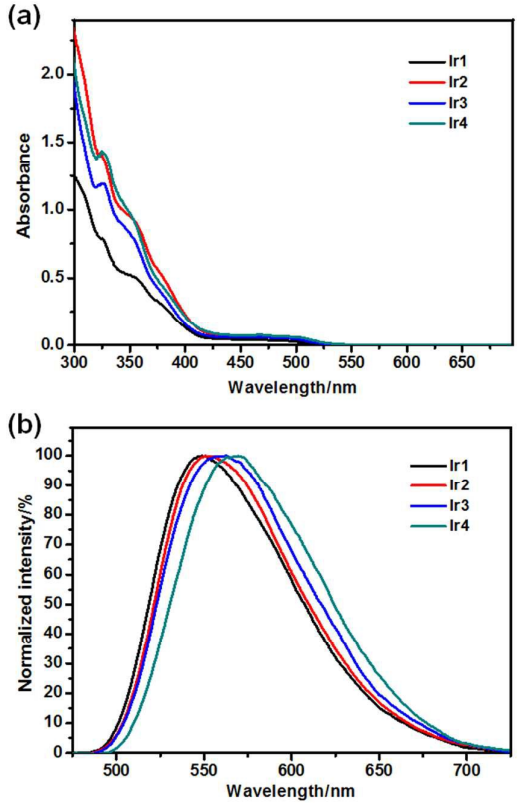

Fig. 3 (a) Absorption spectra and (b) emission spectra of **Ir1-Ir4** (10 μM) in PBS.

Cellular uptake and intracellular localization

The cellular uptake of the complexes by Human cervix

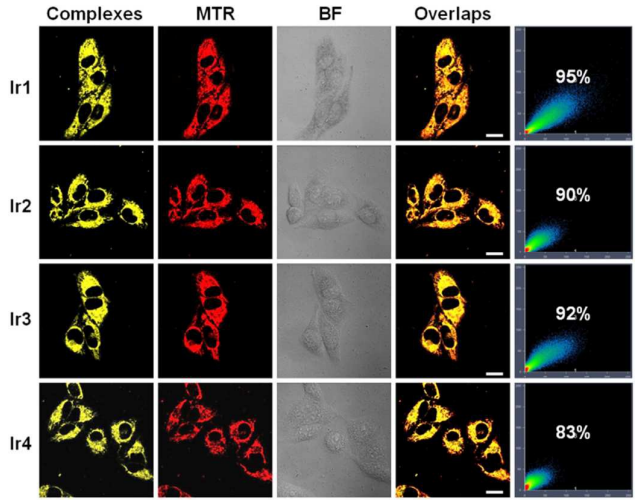

Fig. 4 Confocal images of HeLa cells co-labeled with the complexes (10 μM, 1 h) and the commercial mitochondria imaging agent MTR (50 nM, 0.5 h). The complexes were excited at 405 nm. MTR was excited at 543 nm. The phosphorescence/fluorescence was collected at 550 ± 20 nm and 620 ± 20 nm for the complexes and MTR, respectively. BF: bright field. The 5th column was the Pearson correlation coefficient. Scale bar: 20 μm.

Dalton Transactions Accepted Manuscript

This journal is © The Royal Society of Chemistry 20xx

View Article Online
DOI: 10.1039/C8DT02918K

Published on 07 August 2018. Downloaded by University of Sussex on 8/9/2018 9:27:02 AM.

adenocarcinoma (HeLa) cells was investigated by confocal microscopy. As shown in Fig. S14, with an increasing incubation time, the phosphorescent intensities in the images increased. The intensity of emission of the complexes in cells was saturated at around 60 minutes and the phosphorescence distributed in the cell cytoplasm. The distribution of the complexes was studied *via* co-localization assay with commercial organelle-targeting dyes LysoTracker® Red (LTR), ER-Tracker® Red (ERTR) and MitoTracker® Red (MTR). Low overlaps were found between the location of the complexes and LTR (Fig. S15). The Pearson's correlation coefficients were approximately 70% for the complexes and ERTR (Fig. S16), but the coefficients for the complexes and MTR were more than 80%, even more than 90% for **Ir1** and **Ir3** (Fig. 4). The results suggested the complexes mainly localize in mitochondria. Their mitochondrial localization was further confirmed quantitatively *via* inductively coupled plasma mass spectrometry (ICP-MS) analyses. Mitochondria of the complexes from treated HeLa cells were extracted and the iridium contents of the mitochondria were determined to be 74.7% for **Ir1**, 82.2% for **Ir2**, 76.5% for **Ir3** and 79.4% for **Ir4** (Fig. S17). It has been reported a molecule with a log *P* value between 0 and 5 and a change number above zero would probably target mitochondria.[41,52,53] The log *P* values (Fig. S18) of the cations **Ir1-Ir4** were measured to be 0.322 (**Ir1**), 0.613 (**Ir2**), 0.862 (**Ir3**) and 0.557 (**Ir4**). The combined results pointed out that the complexes were mainly localized in mitochondria.

Cellular uptake mechanisms

Usually, small molecules enter cells through energy-dependent or independent pathways.[54,55] In order to discriminate whether the uptake process utilizes energy, the intracellular phosphorescence of **Ir1-Ir4** at 37 °C and 4 °C were recorded first (Fig. S19). Then cells were pretreated with metabolic inhibitors (2-deoxy-D-glucose and oligomycin) before incubation with the iridium complexes.[56,57] Results showed

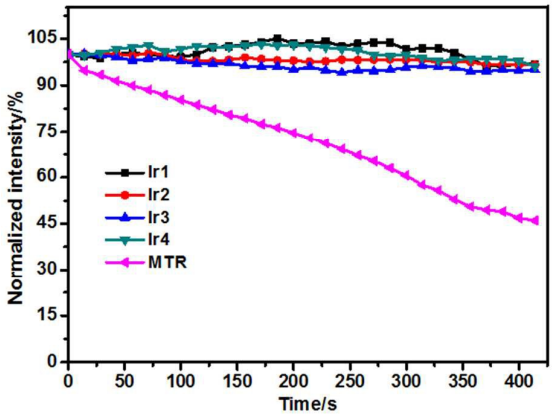

Fig. 5 Quantitative photobleaching results of **Ir1-Ir4** and MTR in HeLa cells under irradiation by a light source (405 nm for the complexes and 543 nm for MTR) of 20.0 mW/cm^2.

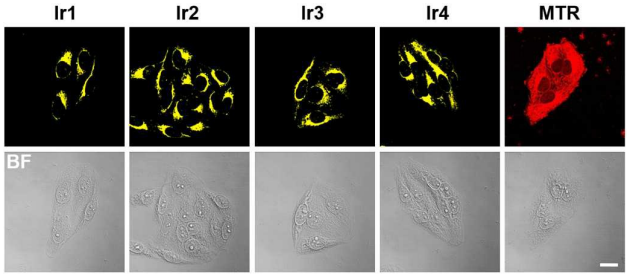

Fig. 6 Confocal phosphorescence/fluorescence images and brightfield (BF) images of fixed HeLa cells incubated with 50 nM MTR for 30 min or 10 μM complexes for 1 h at 37 °C. The complexes were excited at 405 nm. MTR was excited at 543 nm. The phosphorescence/fluorescence was collected at 550 ± 20 nm and 620 ± 20 nm for the complexes and MTR, respectively. Scale bar: 20 μm.

that phosphorescence could still appear clearly in mitochondria at 4 °C, demonstrating the temperature does not affect the entry of the iridium complexes. HeLa cells were pretreated with endocytosis inhibitors (chloroquine and NH_4Cl).[58] Subsequent imaging of the cells showed that **Ir1-Ir4** could still cross the cell membrane in these conditions, thus revealing that the cellular uptake process is not endocytosis. The results infer that all the iridium-based probes in this work share a similar entry mechanism into cells, which is *via* an energy-independent pathway.

Anti-photobleaching in cells

The cellular microenvironment is very complex and different from that in buffer solution.[59] Besides, in order to compare the complexes with commercial dyes, their anti-photobleaching properties in HeLa cells were studied. **Ir1-Ir4** and MTR treated HeLa cells were irradiated under continuous scanning. As shown in Fig. 5 and S20, the fluorescent intensity of MTR finally decreased in half after 30 scans, while the phosphorescence intensities of **Ir1-Ir4** were nearly unchanged

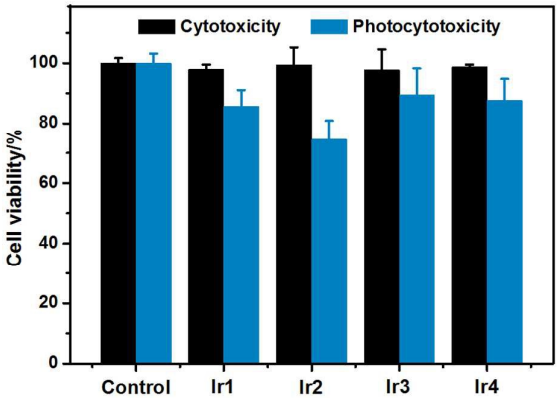

Fig. 7 Viability of HeLa cells incubated with 10 μM of **Ir1-Ir4** for 24 h with or without irradiation (5 J/cm^2, 405 nm).

Dalton Transactions Accepted Manuscript

View Article Online
DOI: 10.1039/C8DT02918K

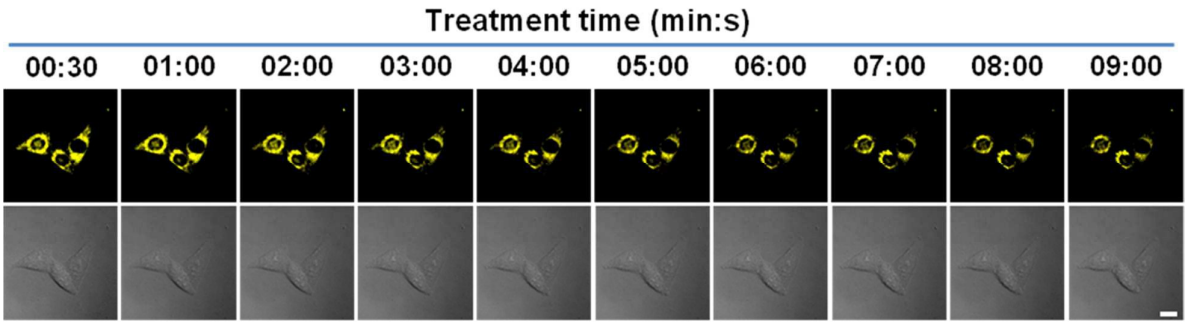

Fig. 8 Real-time imaging of HeLa cells stained with **Ir1** (10 μM) for 1 h at 37 °C, followed by treatment with 30 μM CCCP, with increasing scan time. Phosphorescence images of **Ir1** (upper panel), Brightfield images (lower panels). The complex was excited at 405 nm. The phosphorescence was collected at 550 ± 20 nm. Scale: 20 μm.

compared to initial tests. Dynamic photobleaching changes with time could be seen in Video S1. Results above showed that **Ir1-Ir4** possessed good anti-photobleaching capabilities, and are therefore promising candidates for dynamic tracking in living system.

Imaging in fixed cells

During apoptosis, the mitochondrial membrane potential (MMP) can decrease or even be lost.[18-20] Usually, MMP change would affect the specificity of organic commercial dyes like MTR.[24,27] MMP is totally lost in fixed cells, which can represent the physical status of mitochondria after apoptosis. To study the specificity of mitochondria-targeting, the complexes were used to stain mitochondria in fixed cells and the commercial dye MTR was used as a contrast. As shown in Fig. 6, the whole-cell staining of fixed cells was observed with MTR. However, **Ir1-Ir4** could stain mitochondria in fixed cells as well as living cells, indicating the complexes can target mitochondria even the MMP is lost.

Cytotoxicity measurements

MTT (3-(4,5-dimethylthiazol-2-yl)-2,5-diphenyltetrazoliu bromide) assays were set to study the cytotoxicity of the complexes with HeLa cells. After incubation for 24 h, the complexes did not present significant cytotoxicity in HeLa cells. Photocytotoxicity experiments were made to examine their potential in cellular real-time tracking. Under irradiation of 5 J/cm^2 at 405 nm, HeLa cells subjected to **Ir1**, **Ir3** and **Ir4** still showed viabilities over 80%, while more than 75% cells survived in **Ir2** assay (Fig. 7). The results indicated that the complexes will not interrupt normal biological activities in cells during tracking.

Tracking mitochondrial dynamic during cell apoptosis

Now that **Ir1-Ir4** were shown to have good photostablity, low (photo)cytotoxicity and excellent mitochondrial targeting properties, their application in mitochondrial dynamics tracking during apoptosis was put into practice. Carbonyl cyanide *m*-chlorophenylhydrazone (CCCP) can be used to interrupt the proton gradient across the mitochondrial membrane, leading to MMP decrease and apoptosis.[55] HeLa cells pretreated with **Ir1-Ir4** were exposed to CCCP and the tracking began. The changes of the mitochondrial morphology were shown in Fig. 8 (Video S2). The reticulum structure of the mitochondria was gradually transformed into small and dispersed fragments, indicating the early stages of apoptosis.[21] Similar phenomena (Fig. S20-S22, Video S3-S5) were also found in the experiments with **Ir2-Ir4**. The results displayed the ability of the fluorinated terpyridyl Ir(III) complexes to track mitochondrial dynamics during cell apoptosis.

Conclusions

In summary, a series of phosphorescent fluorinated Ir(III) complexes, **Ir1-Ir4**, were applied to the study of changes in mitochondrial morphology during apoptosis. Tuning of the photophysical properties of the series was demonstrated by the charge in degree of fluorination. The complexes also displayed superior photostability in PBS. Analysis by cellular uptake assay demonstrated the iridium-based probes entry into cells *via* an energy-independent pathway. Co-localization and ICP-MS analyses indicated that **Ir1-Ir4** locate in the mitochondria of HeLa cells. The complexes were also shown to have low cytotoxicities and desirable photobleaching properties. As a result of these excellent characteristics, the complexes were successfully used to track mitochondrial dynamics during apoptosis. We expect our work will facilitate the introduction of fluorine chemistry and terpyridyl Ir(III) complexes for the study of organelles during biological events.

Experimental section

General information

Published on 07 August 2018. Downloaded by University of Sussex on 8/9/2018 9:27:02 AM.
Dalton Transactions Accepted Manuscript

This journal is © The Royal Society of Chemistry 20xx

Please do not adjust margins
View Article Online
DOI: 10.1039/C8DT02918K

Published on 07 August 2018. Downloaded by University of Sussex on 8/9/2018 9:27:02 AM.

The reagents and solvents for chemical synthesis were of analytical grade, and of biological grade for cell experiments. All of them were obtained from commercial sources and used as received unless specified. 2-phenylpyridine, 2-acetylpyridine, 4-fluorobenzaldehyde, 3,4-difluorobenzaldehyde, 2,4,6-trifluorobenzaldehyde and 2,3,5,6-tetrafluorobenzaldehyde were bought from Alfa Aesar (U.S.A.). $IrCl_3 \bullet 3H_2O$ was obtained from Energy Chemical (China). MTT and CCCP were from Sigma Aldrich. LTR, ERTR and MTR were purchased from Invitrogen (U.S.A.). HeLa cells were received from Experimental Animal Center of Sun Yat-Sen University (Guangzhou, China). Dulbecco's modified Eagle medium (DMEM) and fetal bovine serum (FBS) were from Gibco. Ultrapure Milli-Q water was used in all experiments.

Elemental analysis (C, H, N) was performed *via* Elementar Vario EL. Electrospray mass spectra (ES-MS) were acquired from a LCQ system (LCMS-2010A, SHIMADZU, Japan). ^{1}H NMR and ^{19}F NMR spectra were determined on a Bruker AVANCE AV 500 NMR spectrometer, using d_6-DMSO as solvent at room temperature. UV-Vis spectra were recorded on a Perkin-Elmer Lambda 850 spectrophotometer, and emission spectra on a Perkin-Elmer L55 spectrofluorophotometer at room temperature, respectively. Phosphorescent lifetime was measured *via* an Edinburgh FLS-920 combined fluorescence-lifetime and steady-state spectrometer, with excitation source of hydrogen-filled lamp. Phosphorescence quantum yields were performed using $[Ru(bpy)_3]^{2+}$ as reference (0.028 in aerated H_2O).[50] Cell morphologies and imaging were observed through Zeiss LSM 710 laser microscopy system. ICP-MS was conducted on iCAP-RQ inductively coupled plasma mass spectrometer (Thermo Fisher).

Synthesis of Ir(III) complexes Ir1-Ir4

The complexes were synthesized by similar methods according to previous studies.[49,60] Firstly, for the synthesis of the ligand, 4'-(4-fluorophenyl)-2,2':6',2"-terpyridyl (**L1**), a mixture of EtOH (25 mL) , KOH (10 mmol, 0.56 g), 2-acetylpyridine (10 mmol, 1.21 g), 4-fluorobenzaldehyde (5 mmol, 0.620 g) and $NH_3 \bullet H_2O$ (14.5 mL) were added accordingly into a 100 mL round bottom flask and stirred at room temperature overnight. Then the cream white precipitate was filtered and washed with EtOH, water and diethyl-ether three times. The ligand isolated as a white solid was dried and saved for subsequent use.

Secondly, a mixture of **L1** (0.28 mmol, 91.6 mg) and $IrCl_3 \bullet 3H_2O$ (0.32 mmol, 112 mg) in 10 mL ethylene glycol was heated at 180 °C under argon for 30 minutes. The intermediate product was reddish-brown and filtered immediately before washing with EtOH, water and diethyl ether successively. The intermediate (after drying) was further reacted with excess 2-phenylpyridine in ethylene-glycol at 180 °C under argon overnight, until the solution became clear. After cooling to room temperature, the solution was carefully added into saturated NH_4PF_6 solution dropwise. An orange precipitate was formed, isolated by filtration and washed with water and ether three times. The crude product was purified by column chromatography on neutral alumina, using acetonitrile-toluene (v/v: 1:2) as the eluant. The solvent was removed *via* rotary evaporator, and then the purified orange **Ir1** was obtained. The synthesis methods of **Ir2-Ir4** were similar as that of **Ir1**.

[Ir**L1**(ppy)Cl](PF_6) (**Ir1**). Yield: 56.1%. Elemental analysis: calcd (%) for $C_{32}H_{22}ClF_7IrN_4P$: C, 45.00; H, 2.60; N, 6.56. Found: C, 44.77; H, 2.61; N, 6.53. ES-MS (m/z): 709.1 $[M\text{-}PF_6^-]^+$, found: 708.9 $[M\text{-}PF_6^-]^+$. ^{1}H NMR (500 MHz, d_6-DMSO) δ 9.88 (d, *J* = 5.6 Hz, 1H), 9.26 (s, 2H), 8.95 (d, *J* = 8.0 Hz, 2H), 8.50 (d, *J* = 8.2 Hz, 1H), 8.39 (dd, *J* = 8.8, 5.3 Hz, 2H), 8.30-8.21 (m, 3H), 7.94 (d, *J* = 7.9 Hz, 1H), 7.81 (t, *J* = 7.2 Hz, 1H), 7.69 (d, *J* = 5.3 Hz, 2H), 7.60 (t, *J* = 8.8 Hz, 2H), 7.54 (t, *J* = 7.2 Hz, 2H), 6.92 (t, *J* = 7.6 Hz, 1H), 6.75 (t, *J* = 7.9 Hz, 1H), 6.07 (d, *J* = 7.4 Hz, 1H). ^{19}F NMR (470 MHz, d_6-DMSO) δ -67.40, -70.91, -109.86.

[Ir**L2**(ppy)Cl](PF_6) (**Ir2**). Yield: 54.9%. Elemental analysis: calcd (%) for $C_{32}H_{21}ClF_8IrN_4P$: C, 44.07; H, 2.43; N, 6.42. Found: C, 43.85; H, 2.44; N, 6.39. ES-MS (m/z): 727.2 $[M\text{-}PF_6^-]^+$, found: 726.9 $[M\text{-}PF_6^-]^+$. ^{1}H NMR (500 MHz, d_6-DMSO) δ 9.88 (d, *J* = 5.1 Hz, 1H), 9.28 (s, 2H), 8.94 (d, *J* = 8.0 Hz, 2H), 8.49 (m, 2H), 8.27 (m, 4H), 7.94 (d, *J* = 7.2 Hz, 1H), 7.89-7.79 (m, 2H), 7.70 (d, *J* = 5.0 Hz, 2H), 7.55 (t, *J* = 7.2 Hz, 2H), 6.92 (t, *J* = 7.5 Hz, 1H), 6.74 (t, *J* = 6.9 Hz, 1H), 6.06 (d, *J* = 7.7 Hz, 1H). ^{19}F NMR (470 MHz, d_6-DMSO) δ -69.39, -70.91, -135.06, -135.11, -137.18, -137.23.

[Ir**L3**(ppy)Cl](PF_6) (**Ir3**). Yield: 53.8%. Elemental analysis: calcd (%) for $C_{32}H_{20}ClF_9IrN_4P$: C, 43.18; H, 2.26; N, 6.29. Found: C, 42.96; H, 2.27; N, 6.26. ES-MS (m/z): 745.2 $[M\text{-}PF_6^-]^+$, found: 745.0 $[M\text{-}PF_6^-]^+$. ^{1}H NMR (500 MHz, d_6-DMSO) δ 9.87 (d, *J* = 5.2 Hz, 1H), 9.16 (s, 2H), 8.82 (d, *J* = 8.1 Hz, 2H), 8.51 (d, *J* = 8.2 Hz, 1H), 8.29 (t, *J* = 8.6 Hz, 1H), 8.21 (t, *J* = 8.5 Hz, 2H), 7.96 (d, *J* = 7.2 Hz, 1H), 7.82 (t, *J* = 6.6 Hz, 1H), 7.75-7.63 (m, 4H), 7.56 (t, *J* = 6.1 Hz, 2H), 6.94 (t, *J* = 7.9 Hz, 1H), 6.79 (t, *J* = 7.5 Hz, 1H), 6.03 (d, *J* = 7.4 Hz, 1H). ^{19}F NMR (470 MHz, d_6-DMSO) δ -69.40, -70.91, -103.85, -103.87, -103.88, -109.86, -109.87.

[Ir**L4**(ppy)Cl](PF_6) (**Ir4**). Yield: 52.1%. Elemental analysis: calcd (%) for $C_{32}H_{19}ClF_{10}IrN_4P$: C, 42.32; H, 2.11; N, 6.17. Found: C, 42.11; H, 2.12; N, 6.14. ES-MS (m/z): 763.1 $[M\text{-}PF_6^-]^+$, found: 762.9 $[M\text{-}PF_6^-]^+$. ^{1}H NMR (500 MHz, d_6-DMSO) δ 9.87 (d, *J* = 5.1 Hz, 1H), 9.23 (s, 2H), 8.81 (d, *J* = 8.0 Hz, 2H), 8.52 (d, *J* = 8.2 Hz, 1H), 8.32-8.21 (m, 4H), 7.96 (d, *J* = 7.4 Hz, 1H), 7.82 (t, *J* = 7.1 Hz, 1H), 7.73 (d, *J* = 5.5 Hz, 2H), 7.58 (t, *J* = 7.2 Hz, 2H), 6.94 (t, *J* = 7.5 Hz, 1H), 6.79 (t, *J* = 7.0 Hz, 1H), 6.04 (d, *J* = 7.6 Hz, 1H). ^{19}F NMR (470 MHz, d_6-DMSO) δ -69.40, -70.91, -138.08, -138.11, -138.13, -138.16, -141.38, -141.41, -141.43, -141.46.

Cell culture

HeLa cells were seeded in a medium containing 90% DMEM and 10% FBS, then cultured at 37 °C in 5 % CO_2 incubator.

MTT assay

MTT assay was utilized to determine the cell viability of HeLa cells over time after treatment with the iridium-based probes. HeLa cells were seeded in 96-wells plates for 24 h. Then HeLa cells were treated with 10 μM of **Ir1-Ir4** for 1 h in the dark. For the phototoxicity, an LED system was used to irradiate the cells under 405 nm (5 J/cm^2). Then cells in both light and dark assays were incubated in the dark. After 24 h, the cells were

Dalton Transactions Accepted Manuscript

View Article Online
DOI: 10.1039/C8DT02918K

incubated together with MTT solution (20 μL/well, 5 mg/mL) for another 4 hours. Finally, the MTT media was removed and replaced with 200 μL of DMSO in each well. After shaking for 5 minutes, the OD_{595} values were measured with a Tecan Infinite M200 monochromator-based multifunction microplate reader.

Colocalization imaging

After incubation with 10 μM of **Ir1-Ir4** at 37 °C for 1 h, HeLa cells were stained with 50 nm LTR/MTR or 1 μM ERTR for an additional 0.5 h. The cells were rinsed with PBS three times and observed by confocal microscopy. The excitation wavelength of **Ir1-Ir4** was 405 nm, while the three commercial dyes were excited at 543 nm. The emission signals were collected at 550 ± 20 nm for **Ir1-Ir4** and 620 ± 20 nm for LTR/MTR/ERTR.

ICP-MS analysis

HeLa cells were seeded in 10 cm culture plates in 6 mL of DMEM with 10% FBS. After addition and incubation of **Ir1-Ir4** (10 μM) for 1 h at 37 °C, the cells were digested with trypsin (Gibco) and divided into two portions. One sample was subjected to a mitochondrial extraction kit (Beyotime Biotechnology), and the other was the control group. Then each portion was digested in 65% HNO_3 for one day and diluted with water to 2% HNO_3 solution. The content of iridium complexes was determined by ICP-MS.

Cellular uptake mechanism

In temperature tests, the cells were incubated with **Ir1-Ir4** (10 μM) for 1 h at 4 °C and 37 °C, respectively. In metabolic inhibition tests, cells detached from the culture were first incubated with 2-deoxy-D-glucose (50 mM) and oligomycin (5 μM) in PBS for 1 h at 37 °C. For endocytic inhibition, cells were pretreated with NH_4Cl (50 mM), or chloroquine (50 μM) for 30 min. Then the pretreated samples with each inhibitor were treated with **Ir1-Ir4** (10 μM) in fresh media at 37 °C for 1 h. The cells were imaged by confocal microscopy after washing with PBS.

Fixed cells imaging

For fixed cells, 75% EtOH was used to fix HeLa cells for 0.5 h. Then fixed cells were incubated with **Ir1-Ir4** (10 μM, 1 h) or MTR (50 nm, 30 min) at 37 °C. After washed by PBS for three times, fixed cells imaging was performed by confocal microscopy.

Real-time tracking mitochondrial dynamics during cell apoptosis

For real-time tracking, HeLa cells were stained with **Ir1-Ir4** (10 μM) at 37 °C for 1 h, and then washed by PBS for three times. Before imaging, CCCP (30 μM) was added into the plates. Images were taken every 30 s by confocal microscopy. The complexes were excited at 405 nm and the emission signal was measured at 550 ± 20 nm.

Conflicts of interest

There are no conflicts to declare.

Acknowledgements

This work was supported by the National Science Foundation of China (Nos. 21525105, 21471164 and 21778079), the 973 Program (No. 2015CB856301), the Fundamental Research Funds for the Central Universities and China Postdoctoral Science Foundation (No. 2018M630988).

Notes and references

1 B. Fadeel and S. Orrenius, *J. Intern. Med.*, 2005, **258**, 479-517.
2 P. G. Clarke and S. Clarke, *Anat. Embryol.*, 1996, **193**, 81-99.
3 R. A. Lockshin and Z. Zakeri, *Nat. Rev. Mol. Cell Biol.*, 2001, **2**, 545-550.
4 M. M. Metzstein, G. M. Stanfield and H. R. Horvitz, *Trends Genet.*, 1998, **14**, 410-416.
5 B. A. Hay, J. R. Huh and M. Guo, *Nat. Rev. Genet.*, 2004, **5**, 911-922.
6 J. F. Kerr, A. H. Wyllie and A. R. Currie, *Br. J. Cancer*, 1972, **26**, 239-257.
7 J. C. Reed, *Cancer Cell*, 2003, **3**, 17-22.
8 T. G. Cotter, *Nat. Rev. Cancer*, 2009, **9**, 501-507.
9 Q. L. Deveraux and J. C. Reed, *Genes. Dev.*, 1999, **13**, 239-252.
10 D. R. Green and J. C. Reed, *Science*, 1998, **281**, 1309-1312.
11 S. Vyas, E. Zaganjor and M. C. Haigis, *Cell*, 2016, **166**, 555-566.
12 F. Weinberg, R. Hamanaka, W. W. Wheaton, S. Weinberg, J. Joseph, M. Lopez, B. Kalyanaraman, G. M. Mutlu, G. R. Budinger and N. S. Chandel, *Proc. Natl. Acad. Sci. U. S. A.*, 2010, **107**, 8788-8793.
13 M. Leist, B. Single, A. F. Castoldi, S. Kühnle and P. Nicotera, *J. Exp. Med.*, 1997, **185**, 1481-1486.
14 N. J. McCarthy, M. K. Whyte, C. S. Gilbert and G. I. Evan, *J. Cell Biol.*, 1997, **136**, 215-227.
15 T. Hirsch, P. Marchetti, S. A. Susin, B. Dallaporta, N. Zamzami, I. Marzo, M. Geuskens and G. Kroemer, *Oncogene*, 1997, **15**, 1573-1581.
16 G. Lessene, P. E. Czabotar and P. M. Colman, *Nat. Rev. Drug Discov.*, 2008, **7**, 989-1000.
17 J. Xiang, D. T. Chao and S. J. Korsmeyer, *Proc. Natl. Acad. Sci. U. S. A.*, 1996, **93**, 14559-14563.
18 D. R. Green and G. Kroemer, *Science*, 2004, **305**, 626-629.
19 K. Okamoto and J. M. Shaw, *Annu. Rev. Genet.*, 2005, **39**, 503-536.
20 D. Arnoult, *Trends Cell Biol.*, 2007, **17**, 6-12.
21 M. Karbowski and R. J. Youle, *Cell Death Differ.*, 2003, **10**, 870-880.
22 J. L. Perfettini, T. Roumier and G. Kroemer, *Trends Cell Biol.*, 2005, **15**, 179-183.
23 K. Elquss, J. Pakay, M. T. Ryan and C. S. Palmer, *Biochim. Biophys. Acta*, 2013, **1833**, 150-151.
24 Y. Chen, L. Qiao, B. Yu, G. Li, C. Liu, L. Ji and H. Chao, *Chem. Commun.*, 2013, **49**, 11095-11097.
25 Y. Chen, T. W. Rees, L. Ji and H. Chao, *Curr. Opin. Chem. Biol.*, 2018, **43**, 51-57.

Published on 07 August 2018. Downloaded by University of Sussex on 8/9/2018 9:27:02 AM.
Dalton Transactions Accepted Manuscript

This journal is © The Royal Society of Chemistry 20xx

Please do not adjust margins
View Article Online
DOI: 10.1039/C8DT02918K

26 K. Qiu, Y. Chen, T. W. Rees, L. Ji and H. Chao, *Coord. Chem. Rev.*, 2017, DOI: 10.1016/j.ccr.2017.10.022.
27 Y. Chen, L. Qiao, L. Ji and H. Chao, *Biomaterials*, 2014, **35**, 2-13.
28 X. Zhou, F. Su and H. Lu, *Biomaterials*, 2012, **33**, 171-180.
29 Q. Zhao, F. Li and C. Huang, *Chem. Soc. Rev.*, 2010, **39**, 3007-3030.
30 D. Ma, V. P. Ma, D. S. Chan, K. Leung, H. He and C. Leung, *Coord. Chem. Rev.*, 2012, **256**, 3087-3113.
31 Y. Chen, R. Guan, C. Zhang, J. Huang, L. Ji and H. Chao, *Coord. Chem. Rev.*, 2016, **310**, 16-40.
32 C. Caporale and M. Massi, *Coord. Chem. Rev.*, 2018, **363**, 71-91.
33 K. K.-W. Lo and K. K.-S. Tso, *Inorg. Chem. Front.*, 2015, **2**, 510-524.
34 Y. You and W. Nam, *Chem. Soc. Rev.*, 2012, **41**, 7061-7084.
35 K. K.-W. Lo, *Acc. Chem. Res.*, 2015, **48**, 2985-2995.
36 K. Qiu, H. Huang, B. Liu, Y. Liu, P. Zhang, Y. Chen, L. Ji and H. Chao, *J. Mater. Chem. B*, 2015, **3**, 6690-6697.
37 W. Lv, Z. Zhang, K. Y. Zhang, H. Yang, S. Liu, A. Xu, S. Guo, Q. Zhao and W. Huang, *Angew. Chem. Int. Ed.*, 2016, **55**, 9947-9951.
38 Z. Chen, K. Y. Zhang, X. Tong, Y. Liu, C. Hu, S. Liu, Q. Yu, Q. Zhao and W. Huang, *Adv. Funct. Mater.*, 2016, **26**, 4386-4396.
39 T. Huang, Q. Yu, S. Liu, W. Huang and Q. Zhao, *Dalton Trans.*, 2018, **47**, 7628-7633.
40 K. Qiu, Y. Liu, H. Huang, C. Liu, H. Zhu, Y. Chen, L. Ji and H. Chao, *Dalton Trans.*, 2016, **45**, 16144-16147.
41 H. Huang, L. Yang, P. Zhang, K. Qiu, J. Huang, Y. Chen, J. Diao, J. Liu, L. Ji, J. Long and H. Chao, *Biomaterials*, 2016, **83**, 321-331.
42 H. Huang, P. Zhang, K. Qiu, J. Huang, Y. Chen, L. Ji and H. Chao, *Sci. Rep.*, 2016, **6**, 20887.
43 M. C. Z. Kasuya, S. Nakano, R. Katayama and K. Hatanaka, *J. Fluorine Chem.*, 2011, **132**, 202-206
44 Z. Zhang, W. Shen, J. Ling, Y. Yan, J. Hu and Y. Cheng, *Nat. Commun.*, 2018, **9**, 1377.
45 T. Wu, L. Wang, S. Ding and Y. You, *Macromol. Biosci.*, 2017, **17**, 1700114.
46 H. J. Lehmler, *Expert Opin. Drug Deliv.*, 2007, **4**, 247-262.
47 M. Wang, H. Liu, L. Li and Y. Cheng, *Nat. Commun.*, 2013, **5**, 3053.
48 G. Zuo, A. Xie, X. Pan, T. Su, J. Li and W. Dong, *ACS Appl. Nano Mater.*, 2018, **1**, 2376−2385.
49 D. N. Chirdon, W. J. Transue, H. N. Kagalwala, A. Kaur, A. B. Maurer, T. Pintauer and S. Bernhard, *Inorg. Chem.*, 2014, **53**, 1487-1499.
50 K. E. Erkkila, D. T. Odom and J. K. Barton, *Chem. Rev.*, 1999, **99**, 2777-2796.
51 Y. Liu, H. Ma, H. Xu, J. Sun and K. Han, *Int. J. Quantum Chem.*, 2005, **102**, 415-421.
52 R. W. Horobin and F. Rashid-Doubell, *Biotech. Histochem.*, 2013, **88**, 461-476.
53 R. W. Horobin, F. Rashid-Doubell, J. D. Pediani and G. Milligan, *Biotech. Histochem.*, 2013, **88**, 440-460.
54 C. W. Leung, Y. Hong, S. Chen, E. Zhao, J. W. Lam and B. Z. Tang, *J. Am. Chem. Soc.*, 2013, **135**, 62-65.
55 T. Nishikawa, D. Edelstein, X. L. Du, S. Yamagishi, T. Matsumura, Y. Kaneda, M. A. Yorek, D. Beebe, P. J. Oates, H. P. Hammes, I. Giardino and M. Brownlee, *Nature*, 2000, **404**, 787-790.
56 C. A. Puckett and J. K. Barton, *Biochemistry*, 2008, **47**, 11711-11716.
57 K. Y. Zhang, H. W. Liu, T. H. Fong, X. G. Chen and K. K.-W. Lo, *Inorg. Chem.*, 2010, **49**, 5432-5443.
58 J. S. Lau, P. K. Lee, K. H. Tsang, C. H. Ng, Y. W. Lam, S. H. Cheng and K. K.-W. Lo, *Inorg. Chem.*, 2009, **48**, 708-718.
59 K. Qiu, L. Ke, X. Zhang, Y. Liu, T. W. Rees, L. Ji, J. Diao and H. Chao, *Chem. Commun.*, 2018, **54**, 2421-2424.
60 J. Wang and G. S. Hanan, *Synlett*, 2005, **8**, 1251-1254.

Published on 07 August 2018. Downloaded by University of Sussex on 8/9/2018 9:27:02 AM.
Dalton Transactions Accepted Manuscript

View Article Online
DOI: 10.1039/C8DT02918K

Graphical Abstract

A series of phosphorescent fluorinated Ir(III) complexes, which possess low cytotoxicity, excellent photostability and the specificity of mitochondria-targeting, were used for tracking mitochondrial dynamics during apoptosis.

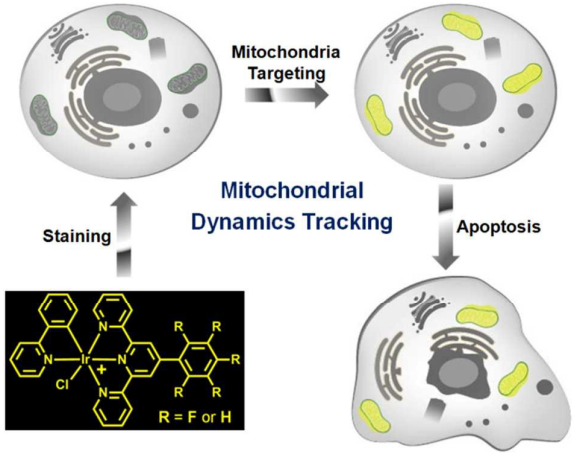

Published on 07 August 2018. Downloaded by University of Sussex on 8/9/2018 9:27:02 AM.

Dalton Transactions Accepted Manuscript